eters of e^2Qq_{zz}/h = 196 kHz and η = 0.18. Although the deuterium quadrupole coupling constants in the microcrystalline phase are larger, the corresponding N–O distances are only slightly longer than found in the crystalline phase (Table VII). In the site of particular interest (N3), the N···O hydrogen bond length in the microcrystalline phase is, at most, 0.1 Å greater than in the crystalline phase. Therefore, the difference in hydrogen bonding to the two phases is small and is unlikely to be the major source of the different ^{15}N chemical shift asymmetry parameters observed in the two phases. Spin–lattice relaxation times of the peptide deuterons in both the monoclinic and triclinic phases were about 15 s, suggesting that all the nitrogen sites are rigid in both crystalline phases.

Discussion

We have shown that a straightforward analysis of ^{15}N–^2H dipolar-coupled ^{15}N line shapes yields precise values of ^{15}N–^2H bond distances as well as the orientation of ^{15}N chemical shift tensor relative to the N–H bond axis (the z axis of the dipolar tensor). The proton-decoupled ^{15}N–^2H dipole-coupled ^{15}N spectra exhibit the ^{15}N–^2H coupling in a straightforward fashion and are simple to analyze because the coupled spins can be treated as an isolated two-spin system. The determination of bond distances from ^{15}N–^1H dipole-coupled ^{15}N spectra requires application of a more complex pulse sequence to eliminate homonuclear proton coupling. The decoupling sequence scales the ^{15}N–^1H coupling, thereby requiring the measurement of the scale factor in order to extract distance information from such spectra.[18] Although double labeling is required to observe the ^{15}N–^2H coupled spectrum, this is readily accomplished because the peptide hydrogen is exchangeable.

The internuclear ^{15}N–^2H bond distances obtained from the analysis of the NMR line shapes are 1.04–1.05 Å in the two crystalline forms of the peptide. These distances are 0.02–0.03 Å greater than typical peptide N–H bond distances obtained from neutron diffraction[19] but agree with bond distances obtained from another NMR study.[18]

Undoubtedly, the NMR and neutron studies yield different values of the N–H bond distance because molecular motions affect the outcome of the two types of experiments in different ways. In particular, librational motions of the ^{15}N–^2H bond reduce the magnitude of the ^{15}N–^2H dipole–dipole coupling. Because the observed (averaged) dipolar coupling is smaller than the static coupling, the value of the internuclear distance obtained from the analysis of the powder line shapes overestimates the bond length. In the case of $Boc(Gly)_3OBz$, the observed coupling yields ^{15}N–^2H bond lengths of 1.04–1.05 Å. However, the observed coupling yields a bond length of 1.02 Å if we assume that the ^{15}N–^2H bond axis undergoes restricted diffusion (rms angle 12–14°) in a cone. We therefore conclude that as a consequence of bond librations the distances obtained from the NMR likely overestimate the ^{15}N–^2H bond length by ca. 0.02 Å.

Because the librational frequencies are much greater than ω_0, these small-amplitude motions do not contribute significantly to spin–lattice relaxation in either the laboratory or rotating frame. Therefore, we observed large values of T_1 and $T_{1\rho}$ for ^{15}N and ^2H nuclei in both crystalline forms of the peptide.

The similarity in ^{15}N–^2H internuclear distances found in the two crystalline forms of the peptide contrasts with the large difference in ^{15}N shift tensor asymmetry parameters obtained in the two crystalline phases. The large differences in unit cell shapes and sizes in the two crystalline phases suggest that a difference in peptide conformation may account for the difference in η. Unfortunately, the unusually large value of η (0.44) was observed for the triclinic phase, which yielded microcrystals that were not suitable for an X-ray structure determination. The ^2H NMR spectra showed that this phase had normal hydrogen bond lengths, so that it is not likely that the large η value is caused by an unusual hydrogen bond. One intriguing possibility is that the large η results from a nonplanar peptide bond in the triclinic phase. Nonplanar peptide bonds have been reported in a number of peptide crystal structures.[20] The principal elements of the ^{15}N shift tensor should be very sensitive to the overlap of the carbonyl carbon and nitrogen π orbitals. To our knowledge, molecular orbital calculations of ^{15}N chemical shift tensor elements have not been carried out. In view of the importance of the peptide bond conformation in determining peptide and protein structure, we hope that this study stimulates further theoretical and experimental work to determine whether the asymmetry of the CSA tensor is correlated with the conformation of the peptide bond.[21]

Registry No. BOC-Gly-Gly-[^2H,^{15}N]Gly-OBzl, 113353-39-2.

Supplementary Material Available: Tables of positional and refined parameters and hydrogen atom parameters (2 pages); listing of observed and calculated structure factors (20 pages). Ordering information is given on any current masthead page.

(18) Roberts, J. E.; Harbison, G. S.; Munowitz, M. G.; Herzfeld, J.; Griffin, R. G. *J. Am. Chem. Soc.* **1987**, *109*, 4163–4169.
(19) Keiter, E. A. Ph.D. Thesis, University of Illinois, 1986.
(20) (a) Mauger, A. B.; Stuart, O. A.; Highet, R. J.; Silverton, J. V. *J. Am. Chem. Soc.* **1982**, *104*, 174–180. (b) Mauger, A. B.; Stuart, O. A.; Ferretti, J. A.; Silverton, J. V. *J. Am. Chem. Soc.* **1985**, *107*, 7154–7163.
(21) Ando, S.; Yamanobe, T.; Ando, I.; Shoji, A.; Ozaki, T.; Tabeta, R.; Saito, H. *J. Am. Chem. Soc.* **1985**, *107*, 7648–7652.

Head-Group Orientation of a Glycolipid Analogue from Deuterium NMR Data

Preetha Ram and J. H. Prestegard*

Contribution from the Chemistry Department, Yale University, New Haven, Connecticut 06511.
Received July 7, 1987

Abstract: A methodology is presented for the conformational analysis of glycolipid head groups in membrane-like environments. The methodology depends on orientational data, in the form of deuterium quadrupolar splittings, obtained in field-ordered liquid crystalline arrays of fatty acid micelles. The orientational data are incorporated into a molecular mechanics program in the form of a pseudoenergy term that minimizes when the molecular conformation satisfies orientational constraints. A minimum in a complete energy function, incorporating both theoretical and experimental constraints, is then sought. Using this approach it has been possible to predict a reasonable conformation for the sugar head group of (*N*-dodecyl)-4-*O*-β-D-galactopyranosyl-D-gluconylamide, a glycolipid analogue, anchored to a micelle surface.

Oligosaccharide moieties of membrane glycoproteins and glycolipids play important roles as receptors for hormones, bacterial toxins, viruses, and other agents which influence cellular function.[1,2] A knowledge of the conformational properties of these oligo-

0002-7863/88/1510-2383$01.50/0

saccharides is thus important in establishing a basis for understanding cell surface phenomena. While there has been a recent upsurge in work on the solution conformations of cell surface oligosaccharides,[3,4] the relationship of solution conformation of oligosaccharides to the conformations as they exist on membrane surfaces remains largely unexplored. High-field NMR methods, which have contributed to the elucidation of solution structure of many macromolecules, are inapplicable in the ordered environments of membrane surfaces, and substantially new methodologies must be developed.

Methodologies based on deuterium NMR have proved useful in the investigation of other membrane components, and it is reasonable to explore the use of these methodologies with oligosaccharides as well.[5-7] Deuterium, a spin 1 nucleus, displays both magnetic field–nuclear magnetic moment interactions and electric field gradient–nuclear quadrupole moment interactions. The former are defined in the laboratory frame by the application of a magnetic field. The latter are defined in the molecular frame by the distribution of electrons in chemical bonds, for example, a C–D bond. In ordered systems, the manner in which the two interactions combine depends on the orientation of the bond relative to a molecular frame and on an order parameter matrix describing the ordering of the molecular frame relative to the magnetic field. For a perfectly ordered system with a single well-defined conformation, the quadrupole interaction leads to two lines for each deuterated site. In systems with an axially symmetric field gradient of magnitude eq, these are split by a quadrupole coupling reduced from the maximum value by an angle dependent factor, $(3\cos^2\theta - 1)/2$.

$$\Delta\nu = \{3e^2qQ/2h\}\{(3\cos^2\theta - 1)/2\} \quad (1)$$

In these expressions, $\Delta\nu$ represents the quadrupolar splitting, θ is the angle between the C–D bond vector and the magnetic field, and eQ is the nuclear quadrupole moment. In systems with internal degrees of freedom, quadrupole splittings are reduced by motional averaging. These additional reductions can be described by one or more order parameters.

Most applications have involved random dispersions of bilayers instead of single oriented crystals. Such systems give rise to a superposition of lines, called a powder pattern, for each site. Resolution of overlapping powder patterns, while possible, is difficult.[8] More definitive results are therefore obtained when multiple sites can be labeled and resolved in oriented rather than dispersed samples.

There has been preliminary work with deuterium NMR. This includes our own work on surface associated mono- and disaccharides and some work of Smith and co-workers on membrane-attached glycolipids.[9,10] In addition to differences in carbohydrates, these studies differ in the means for achieving orientation. The latter experiments were carried out using bilayers ordered between glass plates. Our experiments were performed in liquid crystalline media exhibiting field-induced order. In our early work, as well as that presented here, fatty acid micelles, which display a crude approximation to membrane bilayer surfaces, are used as field-ordered media. However, other systems more closely resembling biological membranes have been shown to exhibit field-induced order,[11] and there is promise of extending these kinds of experiments to these other systems.

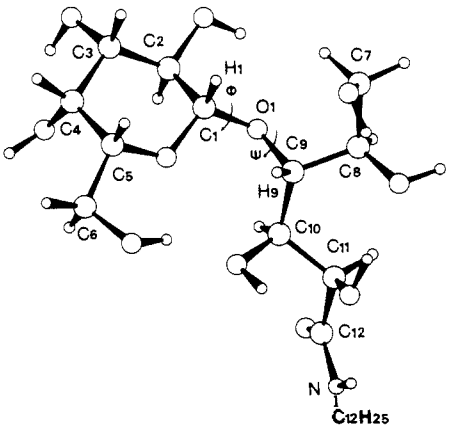

Figure 1. Structure of DLAM showing Φ and Ψ.

Here we extend our previous work using liquid crystals and associated mono- and disaccharides by examining a system where a sugar has been anchored to a micelle, as it would be in a glycolipid. The molecule we use is (*N*-dodecyl)-4-*O*-β-D-galactopyranosyl-D-gluconylamide, or *N*-dodecyllactobionamide (DLAM) (Figure 1). This compound provides a reasonable step toward application of methodology to natural cell surface oligosaccharides in that the dodecyl chain provides a hydrophobic anchor for the hydrophilic lactobionyl group, and the lactobionyl moiety provides a simple oligosaccharide analogue with a number of sites for deuterium labeling. The molecule also has biochemical significance since it has been used as a receptor for lectins.[12]

The extension of our methodology to an anchored system presents several problems. One involves a demonstration that one can achieve adequate resolution to deal with multiply labeled molecules. The other lies in the interpretation of data and the integration of orientational information with constraints imposed by molecular geometry. The methodology we plan to use to integrate orientational data with molecular constraints follows previous work on the solution structure of oligosaccharides and proteins.[13,14] In these works, we used a widely accepted molecular mechanics program[15] to represent our knowledge of molecular interactions as a series of empirical energy terms, and incorporated NMR derived distance constraints in the program in the form of a pseudoenergy function. Here, we introduce orientational constraints as a pseudoenergy function and demonstrate convergence to conformations which are in agreement with experimental data, with molecular bonding effects, and with intuitive expectations of the behavior of amphipathic groups anchored at membrane interfaces.

Theory

Pseudoenergy functions are in no sense real energies and are more appropriately viewed as error functions which minimize when constraints are satisfied. They mimic bonding energy terms in that they minimize when optimal molecular geometry is found. For the orientation data acquired, the pseudoenergy function must display a minimum when the angle between a C–D bond vector and the director axis produces a splitting that matches experimental data. The following is a suitable error function for quadrupolar splitting data:

$$E = W[\{(1 - 3\cos^2\theta)/2\}^2 - (V_{\text{exptl}}/V_{\max})^2]^2 \quad (2)$$

This function depends on the difference between the experimental

(1) Ketis, N. V.; Grant, C. W. *Biochem. Biophys. Acta* **1982**, *689*, 194–202.
(2) McCarry, R. C.; Anderson, R.; Singhal, S. K. *Cell. Immunol.* **1982**, *71*, 293–302.
(3) Sabesan, S.; Bock, K.; Lemieux, R. U. *Can. J. Chem.* **1984**, *62*, 1034–1045.
(4) Yu, R. K.; Koerner, T. A. W.; Scarsdale, J. N.; Prestegard, J. H. *Chem. Phys. Lipids* **1986**, *42*, 27–48.
(5) Blume, A.; Griffin, R. G. *Biochemistry* **1982**, *21*, 6230–6242.
(6) Skarjune, R.; Oldfield, E. *Biochim. Biophys. Acta* **1979**, *556*, 208–218.
(7) Taylor, M. G.; Akiyama, T.; Smith, I. C. P. *Chem. Phys. Lipids* **1981**, *29*, 327–339.
(8) Bloom, M.; Davies, J. H.; Mackay, A. I. *Chem. Phys. Lett.* **1981**, *80*, 198–202.
(9) Tyrell, P. M.; Prestegard, J. H. *J. Am. Chem. Soc.* **1986**, *108*, 3990–3995.
(10) Jarrel, H. C.; Jovall, P. A.; Giziewicz, J. B.; Turner, L. A.; Smith, I. C. P. *Biochemistry* **1987**, *26*, 1806–1811.
(11) Geacintov, N. E.; Van Nostrand, F.; Becker, J. F.; Tinkel, J. B. *Biochim. Biophys. Acta* **1972**, *267*, 65–79.
(12) Sundler, R. *FEBS Lett.* **1982**, *141*, 11–15.
(13) Scarsdale, J. N.; Yu, R. K.; Prestegard, J. H. *J. Am. Chem. Soc.* **1986**, *108*, 6778–6784.
(14) Holak, T. A.; Prestegard, J. H.; Forman, J. H. *Biochemistry* **1987**, *26*, 4652–4660.
(15) Weiner, S. J.; Kollman, P. A.; Nguyen, D. T.; Case, D. A. *J. Comput. Chem.* **1986**, *7*, 230–252.

quadrupolar splitting for a C–D bond, V_{expt}, scaled by the maximum possible quadrupolar splitting in the ordered system, V_{max}, and a quadrupolar splitting calculated from the angle between a trial position of the C–D bond and an averaging axis. W is a weighting function, chosen to appropriately balance the real and pseudoenergy terms. In the final stages of calculation it would be chosen to be large enough to compensate for poorly represented energy terms such as hydrogen bonding and solvation effects. Inherent in the use of this function are the assumptions that the system is axially symmetric and that splittings of all deuterium sites are scaled by the same order parameter.

In order to simplify the implementation, we orient the axis of the acyl chain along the z axis of our coordinate system and constrain it to this position by using a heavily weighted energy function of the form $E = (1 - \cos^2 \theta')$, where θ' is the angle between the chain axis and the z axis. This allows functions such as $\cos \theta$ in expression 2 to be expressed simply as the z component of any normalized C–D bond vector.

The procedure adopted was described in earlier publications from our lab.[13] It involves a preliminary constrained minimization with only bonding and angular energy terms. This allows the program to locate local minima that might be otherwise unattainable owing to intermediate sterically unfavorably conformations. This is followed by normal constrained minimizations, with constraint terms weighted sufficiently to promote convergence to a structure satisfying the NMR data. The molecular mechanics program used here, AMBER,[15] is equipped to handle biomacromolecules, and its force field is in the process of being optimized for oligosaccharide interactions. It employs the Cartesian coordinate energy refinement approach of Lifson and Warshel[16] and uses an energy function similar in spirit to that of Gelin and Karplus.[17]

Materials and Methods

DLAM was synthesized using the procedure of Williams et al.[18] The reaction involves a methanolic hypoiodite oxidation of lactose to lactobionic acid. The acid is subsequently lactonized by repeated addition of methanol and azeotropic removal of water at low pressure and 30 °C. The amide was obtained in good yield (85%) from the reaction of the lactone with *N*-dodecylamine at room temperature. After one recrystallization from methanol, its melting point[18] (143–144 °C) and NMR spectrum were recorded.

The deuteration procedure involved catalytic exchange over Raney nickel.[19] Exchange takes place with the stereospecific replacement of protons that are present in vicinal–CH(OH) groups. DLAM (60 mg), in an inert argon atmosphere, was dissolved in 15 mL of THF and 3 mL of D_2O; 1–2 mL of a packed suspension of Raney nickel, preexchanged with D_2O, was then added, and this reaction mixture was ultrasonicated by direct probe sonication[19] for 20–60 min at 20, 30, 40, or 55°. The reaction mixture was then centrifuged and the supernatant eluted from a silica gel column. Based on the structure, deuteration is expected to occur at sites 2, 3, 4, 7, 7′, 8, 10, and 11, but rates of deuteration at these sites vary considerably because of differences in steric factors and activation energies. We took advantage of differences in activation energies for exchange at each site by choosing a reaction temperature that gave optimum differences in deuteration levels (40 °C) as a basis for spectral assignment. Levels of incorporation at each site were determined by integration of residual peaks in proton NMR spectra.

All proton spectra were acquired on a home-built 490-MHz spectrometer using 90° pulses and a 4-s repetition delay in DMF-d_7/D_2O solvent. Deuterated solvents were obtained from Aldrich Inc., Milwaukee, WI, and Cambridge Isotopes Labs, Woburn, MA. Spectra were acquired in quadrature with sweep widths of 8 kHz with 32K time domain points, weighted with an exponential function yielding 1-Hz line broadening. In most cases normal digital integration routines were used. Spectra were referenced to the terminal methyl resonance at 0.88 ppm. In cases where peaks were not well resolved or belonged to highly second-order multiplets, integrals were obtained by simulation of spectra using a combination of software supplied by Bruker (PANIC) and software written by Kay.[20]

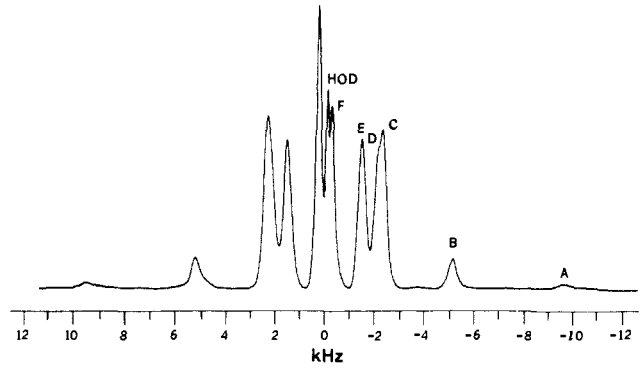

Figure 2. ^{2}H NMR of DLAM in liquid crystalline media.

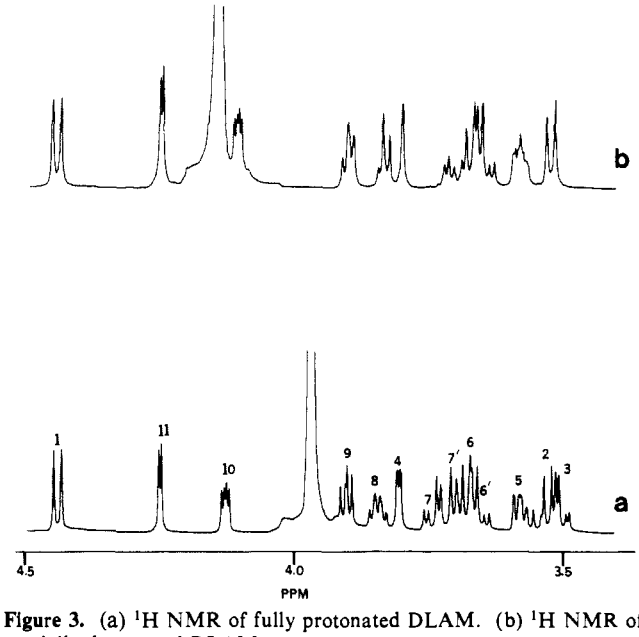

Figure 3. (a) ^{1}H NMR of fully protonated DLAM. (b) ^{1}H NMR of partially deuterated DLAM.

To examine the orientational properties of these molecules, they were dissolved in a liquid crystalline phase composed of potassium laurate, potassium chloride, and water, originally reported by Forrest et al.[21] The phase composition we used (51.6% water, 45.2% potassium laurate, 3.2% potassium chloride) produced homogeneous ordered phases between 30 and 50 °C in the presence of a 11.7-T magnetic field. Deuterium spectra of these phases were acquired in quadrature on a Bruker WM-500 spectrometer operating at 75 MHz; 90° pulses were used with repetition rates of 0.16 s. Data were acquired with 25-kHz sweep width, in 8 K time domain points. Processing included exponential multiplication (20-Hz line broadening) before Fourier transform. Poorly resolved peaks in these spectra were integrated by matching spectral results to spectral simulations of Lorentzian lines of appropriate widths and intensity.

The conformational calculations were performed on a Vax 11/750 using the double precision version of the AMBER energy minimization software as described in the previous section. Both steepest descent and conjugate gradient minimization routines were used and the convergence criterion for the norm of the energy gradient was set to be 0.05 kcal/mol^{-1} Å^{-1}. In the initial stages of the calculations only NMR constraints and bond and angle energy terms were included, with the NMR pseudoenergy weighted sufficient to correspond to 3.9-kcal increase in energy for a 10° departure from experimental constraints when near the maximum value. With these parameters, the average CPU time for convergence of both phases of calculations was 1–2 h.

Results and Discussion

Figure 2 is an example of an oriented deuterium spectrum of DLAM in a potassium laurate micelle. The spectrum shows a number of well-resolved lines. The number of pairs of lines (six plus a pair from residual HOD) is less than the number of sites

(16) Lifson, S.; Warshel, A. *J. Chem. Phys.* **1968**, *49*, 5116–5130.
(17) Gelin, B.; Karplus, M. *Biochemistry* **1979**, *18*, 1256–1262.
(18) Williams, T. J.; Plessas, N. R.; Goldstein, I. J.; Lönngren, J. *Arch. Biochem.* **1979**, *195*, 145–151.
(19) Cioffi, E. A.; Prestegard, J. H. *Tetrahedron Lett* **1986**, *27*, 415–416.
(20) Kay, L. K.; Prestegard, J. H. *J. Magn. Reson.* **1986**, *68*, 515–525.
(21) Forrest, B. J.; Reeves, L. W. *Chem. Rev.* **1981**, *81*, 1–13.

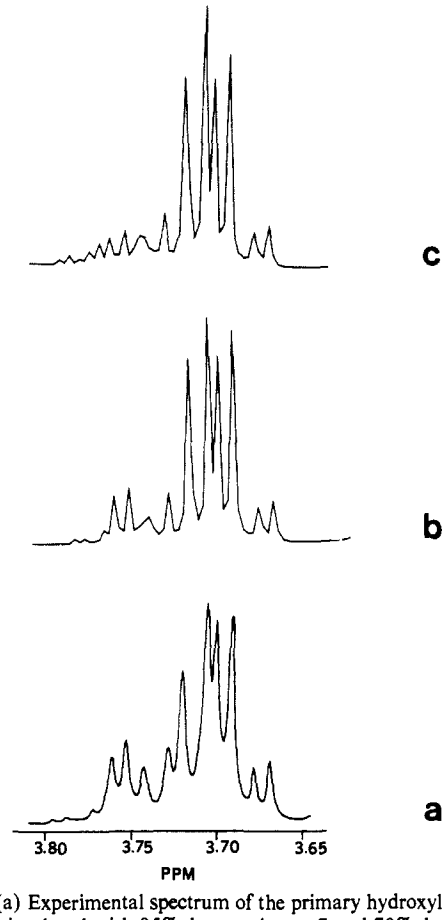

Figure 4. (a) Experimental spectrum of the primary hydroxyl region. (b) Spectrum simulated with 85% deuteration at 7 and 70% deuteration at 7′. (c) Spectrum simulated with 70% deuteration at 7 and 85% deuteration at 7′.

that could undergo significant deuteration, as it should be. To make use of the information in the deuterium spectrum, we need to assign the lines to specific deuteration sites. It is clear that there is considerable variation in the intensities of the different peaks. This correlates directly with variations in the extent of deuteration. Close examination of the proton spectra of the fully protonated glycolipid, and comparison to a proton spectrum of a partially deuterated sample, allows identification of deuterated sites and quantification of deuteration levels. An example is shown in Figure 3. The proton spectrum has been assigned by a 2D-COSY experiment and is labeled in accordance with these assignments. Some of the changes in going from the fully protonated to the partially deuterated spectrum are easily interpretable and quantifiable. For example, consider the H2 and the H3 multiplets which overlap in the upfield region. On deuteration a simple doublet remains, indicating nearly complete deuteration of one site. This doublet region integrates to one proton, indicating <5% deuteration of the other site. The magnitude of the coupling of the remaining peak and the retention of the doublet for H1 at 4.45 ppm, with the same coupling, indicates that it is H3 that is deuterated.

Other areas are not as well resolved and require more careful analysis. Figure 4a shows an expansion of the region containing the H6, H6′, H7′, and H7. Integration of the entire region shows the loss of 1.65 protons. Selectivity rules based on prior extensive deuteration studies of galactopyranosides suggest that H6 and H6′ will not be catalytically exchanged. Residual proton intensity must therefore be divided between 7 and 7′. This multiplet region is also affected by a small level of deuteration at 8. If we assume that incorporation at one site occurs independent of other sites, the partially deuterated spectrum will be a superposition of spectra from six distinct deuterated species. We carried out an analysis by simulating spectra for various species and summing them in appropriate proportions. Chemical shifts and coupling constants

Table I. Deuteration Levels (%)

^{1}H assignment	level from ^{1}H NMR	^{2}H assignment	level from ^{2}H NMR
10	10	A[a]	8
8	28	B	25
7	85	C	85
4	42	D	45
3	93	E	97
7′	70	F	70

[a] Tentative assignment.

Table II. Assignment of Quadrupolar Splittings to Specific C-D Sites in DLAM

deuterium site	C-D bond	quadrupolar splitting (kHz)
A	10[a]	18.5
B	8	10.4
C	7	4.7
D	4	4.5
E	3	3.0
HOD	HOD	0.3
F	7′	0.5

[a] Tentative assignment.

used in the simulation were first derived by fitting the fully protonated spectrum using the Bruker iterative simulation program PANIC and then adjusting chemical shifts for isotope effects.[22] Simulations using different proportions of deuteration at 7 and 7′ are shown in Figure 4, b and c. Figure 4b shows simulated spectra of the region having 85% deuterium at 7 and 70% deuterium at 7′. Figure 4c shows simulated spectra with 70% deuteration at 7 and 85% at 7′. It is clear that Figure 4b gives a better fit. Table I summarizes deuteration levels at various sites obtained by procedures such as these.

Peaks in deuterium spectra were also integrated. Again, simulation of the deuterium spectrum was required because of extensive overlap. The pairs of peaks labeled C and D overlap quite completely. However, one of the splittings changes more with temperature than the other, and simulations at several temperatures were used to improve the reliability of integrations.

Table I also lists the deuterium levels as calculated from simulation of deuterium peak areas. Correlation of areas from assigned proton spectra and unassigned deuterium spectra were used to assign quadrupole splittings as shown in Table II. Chemical shift information, derived from the offsets of the centers of the quadrupolar doublets, provides additional information. For example, in the case of the pairs C and D, the chemical shifts information extracted from the deuterium spectra is consistent with the assignments. Except for the assignment of doublet A to proton H10, we consider the assignments to be reliable. H10 is difficult to integrate because of its position on the side of the residual HDO peak in the proton spectrum of the partially deuterated sample. The low level of deuteration (10%) also increases the possibility that the doublet A in the deuterium spectrum could arise from a highly deuterated chemical contaminant.

Assigned deuterium splittings were used in a search for a head-group orientation that would be consistent with observed splittings. As detailed in the Introduction, we employed a pseudoenergy representation of the experimental splittings and a molecular mechanics representation of the molecular geometry. Inherent in most molecular mechanics calculations is the problem of local minima. Commonly employed energy minimization routines cannot distinguish local minima from the global minimum and, therefore, halt at the first local minimum rather than continuing the minimization in the direction of the lowest point in the energy surface. Our approach to this problem is to initially weight NMR constraints heavily in an attempt to simplify the potential energy surface and then to run the minimizations from several starting geometries to more fully explore the surface. Both the glycosidic bond angles and the hydrophilic spacer region

(22) Saur, W.; Crespi, H. L.; Katz, J. J. *J. Magn. Reson.* **1970**, *2*, 47–49.

Table III. AMBER Minimized Structures

	(γ,ω,χ)	initial (Φ, Ψ)	final (Φ, Ψ)	energy (kcal)	θ (H8, H4, H3)	normalized splitting[a] H4, H3	rms deviation
			Initial (γ,ω,χ) = (180,180,180°)				
1	−130, −170, 142	60, 0	65, −13	4.35	93, 47, 49	0.37, 0.28	0.04
2	−129, −179, 158	−60, 0	−30, −30	1.56	93, 47, 118	0.40, 0.34	0.05
3	−124, 179, 162	180, 0	175, 1	−4.98	93, 46, 48	0.47, 0.35	0.05
4	−123, 173, 179	0, 120	−5, 187	1.42	91, 48, 116	0.32, 0.41	0.11
5	−95, −166, 126	180, 180	84, −46	1.23	93, 113, 50	0.56, 0.25	0.10
6	−96, −170, 134	60, −60	79, −52	1.02	91, 113, 64	0.56, 0.41	0.12
7	−59, −145, −169	60, 60	27, −18	7.35	92, 47, 62	0.38, 0.36	0.06
			Initial (γ,ω,χ) = (180,60,−60°)				
8	−152, 68, −54	60, 0	54, 10	4.93	89, 115, 61	0.45, 0.31	0.02
9	−162, 81, −76	−60, 0	−27, −24	5.97	89, 135, 118	0.50, 0.33	0.06
10	−161, 74, −45	180, 0	165, 21	7.86	88, 133, 132	0.42, 0.35	0.04
11	−133, 60, −61	0, 120	61, 86	10.87	89, 67, 47	0.53, 0.39	0.10
12	−133, 59, −61	180, 180	61, 85	10.93	89, 66, 47	0.52, 0.39	0.10
13	−160, 70, −41	60, −60	28, 10	−1.23	87, 134, 62	0.44, 0.36	0.05
14	−153, 68, −69	60, 60	113, 31	7.04	86, 114, 63	0.51, 0.41	0.10

[a] Scaled by the H8 splitting. Experimental ratio = 0.34, 0.29.

connecting the hydrocarbon chain to the sugar head group, C11–C10–C9–C8, are sources of torsional flexibility that can be used to generate starting conformations. There are a total of five torsionally flexible bonds, and even with only three local minima per torsion, a very large number of starting geometries could be explored. We explored 24 distinct starting structures using some discretion in excluding those which had severe steric overlap or directed the hydrophilic head group back along the hydrocarbon chain. Quadrupolar constraints for only H3, H4, and H8 were used. Those for H7 and H7′ were not used because of the likelihood of averaging of splittings by internal rotations around the C7–C8 bond. That for H10 was not included because of the lack of reliability in this assignment.

The results of these calculations are summarized in Table III. We have restricted our summary to conformations having the most probable conformations for the interfacial region of the hydrophilic head group—carbons 11 through 9. We have included relatively little information about this region in our calculations but can exclude many of the resulting conformations based on severe inconsistencies of geometry with vicinal proton–proton coupling constants observed in solution.

In Table III, conformations are partially characterized by the angles defining the glycosidic linkage, three variable angles in the hydrophilic spacer region, and the angles of the of the C–D bond in the terminal ring relative to the acyl chain axis. The dihedral angles Φ (H1–C1–O1–C9) and Ψ (C1–O1–C9–H9) define the glycosidic bond, and the dihedral angles γ (N–C12–C11–C10), ω (C12–C11–C10–C9) and χ (C11–C10–C9–O9) define spacer geometry. These angles are zero when eclipsed and positive when the farthest removed bond is rotated clockwise. Both initial angles and final angles are shown. The various starting structures do not converge to a common solution as one might hope. The orientational pseudopotential is more complex than the one we used to represent distance constraints in our previous work[23] and may lead to more severe local minima problems. Note, however, that the minimization procedure is capable of producing quite large departures from initial geometries. Angle Φ changes by nearly 120° in structure 12 and angle Ψ changes by more than 120° in minimization 5. Also there are examples of convergence to similar structures from distinct starting geometries, for example, the pairs 8 and 13 and 5 and 6.

The viability of various conformers can be evaluated by considering both agreement with ^{2}H NMR data and the molecular energy of the final structure. The angles, θ, each correspond to a predicted normalized quadrupole splitting. The root-mean-square (rms) deviations from experimental values are given in the final column of Table III. It is apparent that the minimization scheme has succeeded in locating structures which satisfy the NMR constraints excellently. An rms deviation of 0.02 corresponds to an error in quadrupole splitting of 200 Hz, a number comparable to the precision of our measurements. If we consider increases in rms deviations of more than a factor of 2 unacceptable, and consider structures within 10 kcal of the lowest energy structure, then two possible structures result, structures 1 and 8. These two structures have similar energies, which are in both cases approximately 9 kcal above that of the apparent global energy minimum, structure 3. These energy differences at first seem quite high. However, we must remember that among other things, solvent interactions and hydrogen bonding to the solvent are not well represented in our calculations. The absence of two to three hydrogen bonds to solvent could give rise to energy discrepancies of this amount. Structure 3 does show an unusual number of intramolecular hydrogen bonds.

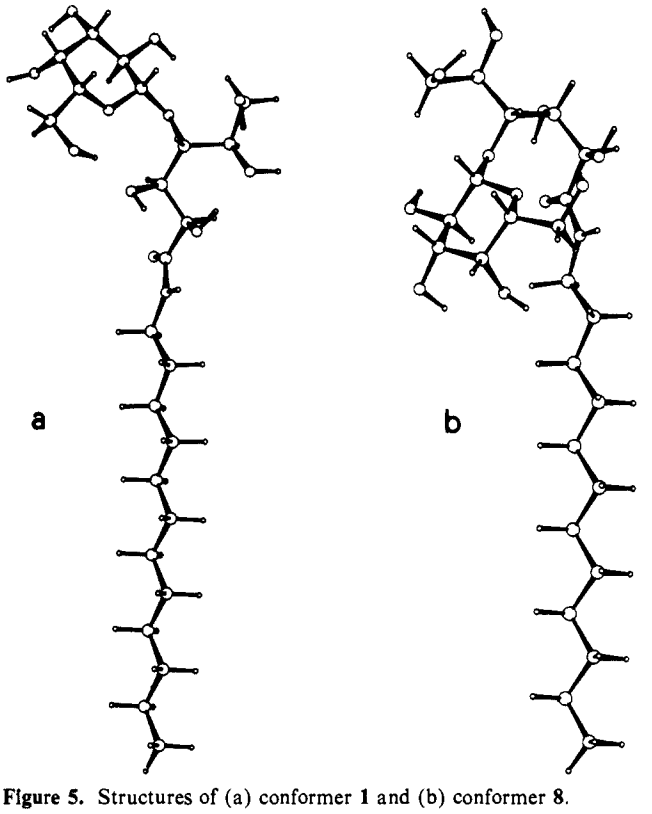

Figure 5. Structures of (a) conformer **1** and (b) conformer **8**.

Both structures, 1 and 8, have Φ and Ψ within 15° of an average Φ, Ψ of 60°, 0°, but present different hydrophilic spacer conformations. The spacer geometry of structure 8 is less probable because it directs the head group back along the hydrocarbon chain. We, therefore, consider 1 the most likely conformation.

(23) Scarsdale, J. N.; Ram, P.; Yu, R. K.; Prestegard, J. H. *J. Comput. Chem.* in press.

It is shown in Figure 5 along with conformation 8.

Our results may be compared with both ab initio results and results recently published by Smith and co-workers.[10] Ab initio calculations in fact suggest preferences for the Φ, Ψ combination of 50°, 0° that arises as the preferred geometry in our results.[24] This enhances confidence in our work in the ab initio calculations. Using phospholipid bilayers oriented between glass plates, Smith and co-workers, investigated the conformational properties of a deuterated 1,2-di-*O*-tetradecyl-3-*O*-(β-D-glucopyranosyl)glycerol. The conformations they prefer are similar to ours in several respects. The sugar head group was found to be extended away from the bilayer surface. The angle between the C1–O1 bond and the acyl chain director, which is related to Ψ, lies between 156 and 173°. The corresponding angle in conformation 1 is calculated to be 126°. Smith and co-workers are not able to settle on one value for the angle corresponding to Φ out of the four possibilities they list, though they tend to favor the lower values of Φ. Our value of Φ would be 60°. The glycolipids studied are, of course, not identical. One difference is in the nature of the monosaccharide, glucose in Smith's glycolipid and galactose in ours. The two monosaccharides are different in the configuration at C4, where galactose has an axial hydroxyl instead of an equatorial hydroxyl group. This difference is spectroscopically useful, because in galactose the C–D bond at the 4 position is not collinear with the C–D bond at 3, thus yielding an additional piece of conformational information. The different hydroxyl orientation may also be in part responsible for the structural variations observed.

The other difference in DLAM is the existence of a hydrophilic spacer region. The presence of a hydrophilic spacer region would imply an increased level of flexibility compared to a direct attachment of the sugars to the glycerol backbone. Implicit in our treatment is the assumption of a single-order parameter scaling down all the deuterium splittings and the assumption of overall rigidity of the molecule. This assumption of molecular rigidity is certainly very valid in the sugar ring region but it is less likely to be so in the hydrophilic spacer region. Variations of the deuterium splittings with temperature provide one test of this assumption. If separate order tensors exist for the ring and spacer region, they are likely to have different temperature dependencies. Splittings for H8, H4, and H3 scale identically as a function of temperature. This adds credence to the use of a single-order parameter to scale both ring C–D vectors and the C–D vector in the hydrophilic spacer region.

It may be possible in the future to relax these assumptions by inclusion of more data, perhaps from proton–dipolar splittings or through-bond scalar coupling. For the time being, a methodology has been presented that combines experimentally derived information, in the form of deuterium NMR quadrupolar splittings with a molecular mechanics program, to arrive at a reasonable conformation for glycolipid head group in a membrane-like environment. This provides a useful means of investigating properties of this very important class of molecules.

Acknowledgment. We thank J. N. Scarsdale for his advice on the implementation of the pseudoenergy potential and L. E. Kay for his assistance in the proton simulations. This research was supported by grants from the National Institutes of Health (GM 191035 and GM 33225), and benefited from instrumentation provided through shared instrumentation program of the Division of Research Resources of the National Institutes of Health (RR 02379).

Registry No. DLAM, 69313-68-4.

(24) Jeffrey, G. A.; Pople, J. A.; Radom, L. *Carbohydr. Res.* **1972**, *25*, 117–131.

Heteronuclear Filters for Two-Dimensional ^{1}H NMR. Identification of the Metal-Bound Amino Acids in Metallothionein and Observation of Small Heteronuclear Long-Range Couplings[1]

Erich Wörgötter,[†,§] Gerhard Wagner,[†,∥] Milan Vašák,[‡] Jeremias H. R. Kägi,[‡] and Kurt Wüthrich*[†]

Contribution from the Institut für Molekularbiologie und Biophysik, Eidgenössische Technische Hochschule-Hönggerberg, CH-8093 Zürich, Switzerland, and Biochemisches Institut der Universität Zürich, Winterthurerstrasse 190, CH-8093 Zürich, Switzerland.
Received July 20, 1987

Abstract: The use of heteronuclear filters for editing of two-dimensional homonuclear ^{1}H NMR experiments is illustrated with studies of [$^{113}Cd_7$]-metallothionein. The previously described X-filter and X(ω_2)-half-filter are employed with an improved phase-cycling scheme to identify the amino acid residues bound to ^{113}Cd. The paper describes the first realization of a 2X-filter, which selects for protons with nonvanishing spin–spin couplings to two X spins and thus presents a new criterion for direct identification of bridging cysteines in metallothioneins. It is further demonstrated that two-dimensional ^{1}H correlation experiments (COSY) recorded with heteronuclear filters enable the identification of small heteronuclear long-range spin–spin couplings, which are otherwise difficult to observe.

During the period 1979–1982, the method of sequential resonance assignments in biopolymers was introduced for proteins[2] and subsequently adapted also for nucleic acids.[3] This technique can rely entirely on homonuclear ^{1}H NMR, provided that sufficiently well-resolved ^{1}H NMR spectra are available.[4] For a variety of small proteins the sequential assignment method ef-

[†] Eidgenössische Technische Hochschule-Hönggerberg.
[‡] Universität Zürich.
[§] Present address: Biochemie GmbH, A-6250 Kundl, Austria.
[∥] Present address: Institute of Science and Technology, Biophysics Research Division, University of Michigan, Ann Arbor, MI 48109.

(1) Abbreviations used: NMR, nuclear magnetic resonance; ppm, parts per million; 2D, two-dimensional; COSY, 2D correlated spectroscopy; TOCSY, 2D total correlation spectroscopy; NOESY, 2D nuclear Overhauser and exchange spectroscopy; RELAYED-COSY, 2D relayed coherence transfer spectroscopy; E.COSY, 2D exclusive correlated spectroscopy; MT2, metallothionein isoprotein 2 from rat liver; TSP, (trimethylsilyl)propionic acid sodium salt.

0002-7863/88/1510-2388$01.50/0